Journal of Neurology (2022) 269:4102–4109
https://doi.org/10.1007/s00415-022-11024-y

ORIGINAL COMMUNICATION

Epilepsy related to focal neuronal lipofuscinosis: extra-frontal localization, EEG signatures and GABA involvement

Valerio Frazzini[1,2,3] · Bertrand Mathon[2,3,4] · Florian Donneger[2,7,8] · Louis Cousyn[1,2,3] · Aurélie Hanin[2] · V.-H. Nguyen-Michel[1] · Claude Adam[1] · Virginie Lambrecq[1,2,3] · Sophie Dupont[1,3,5] · Jean Christophe Poncer[2,7,8] · Franck Bielle[2,3,6] · Vincent Navarro[1,2,3]

Received: 11 October 2021 / Revised: 7 February 2022 / Accepted: 11 February 2022 / Published online: 7 March 2022

Abstract

Focal neuronal lipofuscinosis (FNL) is an uncommon epileptic disorder related to an excess of lipofuscin accumulation within dysmorphic-appearing neurons (DANs), whose epileptogenic mechanisms are still poorly understood. It shares some clinical and neuroimaging similarities with focal cortical dysplasia of type IIb (FCDIIb), but it represents a different pathological entity. Here, we identified two patients with FNL among a 10-year cohort of 323 patients who underwent neurosurgery for a focal pharmacoresistant epilepsy. We describe the electroclinical, metabolic and neuropathological features of both patients with FNL who benefited from a comprehensive presurgical investigation. While the previous reports showed frontal lobe localization of the lesion, FNL was identified in the temporal lobe, in one of our patients. EEG investigations in both patients showed striking focal and rich interictal activity resembling that described in FCDIIb. Besides focal intraneuronal lipofuscin accumulation, the neuropathological analysis demonstrated that somata of DANs were surrounded by a large amount of GABAergic presynaptic buttons, suggesting the involvement of interneurons in the epileptogenicity of FNL. To further explore the role of GABAergic transmission in the generation of epileptiform activity in FNL, we performed in vitro multi-electrode array recordings on the post-surgery tissue from one patient. Spontaneous interictal-like discharges (IILDs) were identified only in the restricted area displaying the highest density of lipofuscin-containing DANs, suggesting a close correlation between the density of lipofuscin-containing neurons and epileptogenicity. Moreover, IILDs were blocked by the GABAA receptor antagonist gabazine. All together, these findings showed how GABA signaling may contribute to the generation of interictal-like activity in FNL tissue.

Keywords Lipofuscinosis · Focal seizures · SEEG · Dysmorphic appearing neurons · Focal cortical Dysplasia · MEA · GABA

Abbreviations

DANs	Dysmorphic-appearing neurons
FCDIIb	Focal cortical dysplasia of type IIb
FLE	Frontal lobe epilepsy
FNL	Focal neuronal lipofuscinosis
STG	Superior temporal gyrus
MEA	MultiElectrode Array

Franck Bielle and Vincent Navarro contributed equally to this work.

✉ Vincent Navarro
vincent.navarro@aphp.fr

[1] Epilepsy Unit, Department of Neurology and EEG Unit, Department of Clinical Neurophysiology, AP-HP, Pitié Salpêtrière Hospital, Reference Center for Rare Epilepsies, 75013 Paris, France

[2] Paris Brain Institute, ICM, INSERM, CNRS, 75013 Paris, France

[3] Sorbonne Université, 75013 Paris, France

[4] Department of Neurosurgery, AP-HP, Pitié Salpêtrière Hospital, 75013 Paris, France

[5] Rehabilitation Unit, AP-HP, Pitié-Salpêtrière Hospital, Paris, France

[6] Department of Neuropathology, AP-HP, Pitié Salpêtrière Hospital, 75013 Paris, France

[7] Inserm UMR-S 1270, 75005 Paris, France

[8] Institut du Fer À Moulin, 75005 Paris, France

Introduction

Focal neuronal lipofuscinosis (FNL) corresponds to an excess of lipofuscin accumulation within dysmorphic-appearing neurons (DANs) and was described as the pathological hallmark of a distinct type of pharmaco-resistant frontal lobe epilepsy (FLE) [1, 2]. While FNL shares some clinical and neuroimaging features with focal cortical dysplasia of type IIb (FCDIIb), it represents a different neuropathological entity currently described in seven patients [1, 3]. To date, it is still unclear if FNL displays peculiar ictal or interictal electrophysiological features and little is known about the basis of its epileptogenicity. Here, we describe the electroclinical, metabolic and neuropathological features of two patients with focal pharmaco-resistant epilepsy due to FNL who benefited from a comprehensive presurgical investigation. Post-surgical specimen from one patient was further explored using multi-electrode array recordings in vitro to explore the microscopic organization of the locally generated epileptiform activity. The goal of the study is to offer a multilevel description of this challenging epileptogenic pathology with particular emphasis on the relationship between neurophysiological and neuropathological features.

Methods

We screened all patients who underwent epilepsy surgery between January 2010 and December 2020 in the Pitié-Salpêtrière Hospital and for which neuropathological examinations were available. On a total of 323 patients, we identified 2 patients whose histological examination revealed microscopic abnormalities compatible with FNL. Both patients underwent a complete presurgical evaluation in the Epileptology Unit of the Pitié-Salpêtrière Hospital. It included 3 T brain MRI, 27-electrode long-term video-EEG recordings (MicroMed System, Italy) and interictal 18FDG-PET. Interictal and ictal (SISCOM) Tc-99 m-HMPAO SPECT evaluation were performed in both patients. For patient 1, we conducted an intracerebral SEEG investigation exploring the right temporal, parietal and occipital lobes. Nine intracerebral electrodes (AdTech®) were inserted using the robotic ROSA® device (Medtech). Signals were continuously and synchronously recorded at 4 kHz using a hardware filter at 0.01 Hz (Atlas Recording System; NeuraLynx, Tucson, AZ, USA). Post-implantation electrode locations were based on a pre-implantation 3 T 3D-MRI, post-implantation 1.5 T 3D-MRI and CT scan, integrated using the Epiloc toolbox, an in-house developed plugin for the 3D-Slicer visualization software. The study design and report are in accordance with the STROBE statement [4].

Neuropathology

After surgery, brain specimens were formalin-fixed and paraffin-embedded. Three micrometers-thick tissue sections were studied by hematoxylin–eosin, Periodic Acid Schiff (PAS) and Luxol blue stainings or were processed for immunostainings by a fully automated stainer Ultra (Ventana, Roche) using diaminobenzidine as a chromogen and the following primary antibodies and dilutions: monoclonal mouse anti-non phosphorylated neurofilament SMI32 (Biolegend, 1/1000), mouse monoclonal anti-p62 (Becton Dickinson, 1/500), polyclonal rabbit anti-glutamate decarboxylase 65 & 67 (Sigma, 1/3000).

Human tissue and multi-electrode recordings

A written consent was obtained for the in vitro study, according to a procedure validated by the national ethical committee (TIPI project, INSERM C16-16). Cortical specimens collected in the operating room were immediately transported in ice-cold (0–4 °C), oxygenated solution (O2/CO2 95/5%), containing (in mM): N-methyl-d-glucamine 93, KCl 2.5, NaH2PO4 1.2, NaHCO3 30, HEPES 20, D-glucose 20, ascorbic acid 5, sodium pyruvate 3, MgSO4 10 and CaCl2 0.5 (300–310 mOsm, pH 7.4) and transported within 15 min to the laboratory. Transverse cortical slices (400 µm thick) were prepared in the same solution using a vibratome (HM650V, Microm). They were maintained at 37 °C in an interface chamber containing artificial cerebrospinal fluid (ACSF) composed of (in mM): D-glucose 10, KCl 3.5, NaHOC3 26, NaH2PO4 1.25, NaCl 126, CaCl2 1.6 and MgCl2 1.2 (290 mOsm), equilibrated with 5% CO2 in 95% O2. Multielectrode array recordings were performed using a MEA2100 station (Multi Channel Systems) equipped with a 120-microelectrode array chamber (12 × 12 layout, 30 µm titanium nitride electrodes spaced 100 µm). Slices were maintained in the recording chamber using a home-made platinum-nylon harp and superfused with pre-warmed (37 °C) oxygenated ACSF at a rate of 6 ml/min. Slices were imaged using a video-microscope table (MEA-VMT1, Multi Channel Systems) to register the location of electrodes with respect to the slice. Extracellular signals were acquired at a sampling rate of 10 kHz and post-hoc filtered with a low pass Bessel filter (order 2; 40 Hz) using Multi Channel Experimenter (MultiChannelSystems). Analyses were performed offline using homemade software (Matlab, The Mathworks).

Results

Clinical presentation

Patient 1, a 24-year-old woman, suffered from focal epilepsy since the age of 12. Seizures consisted of dizziness and spatiotemporal disorientation, followed by loss of awareness and atonia, sometimes associated with falls. Patient 2, a 30-year-old woman, developed focal seizures since the age of 3 months. A mild right hemiplegia appeared during the second year of life. Seizures were controlled by pharmacological treatment until the age of 26, then the patient experienced a progressive increase in seizure frequency. Seizures usually consisted of paresthesia of the right hemi-body, including the face, followed by hypertonic contraction and then clonus of the upper limb. Awareness was preserved.

Structural and metabolic imaging

In patient 1, brain MRI was normal (Fig. 1a, left). Brain ^{18}FDG-PET found a right temporal hypometabolism including the lateral cortex, up to the parieto-temporal junction

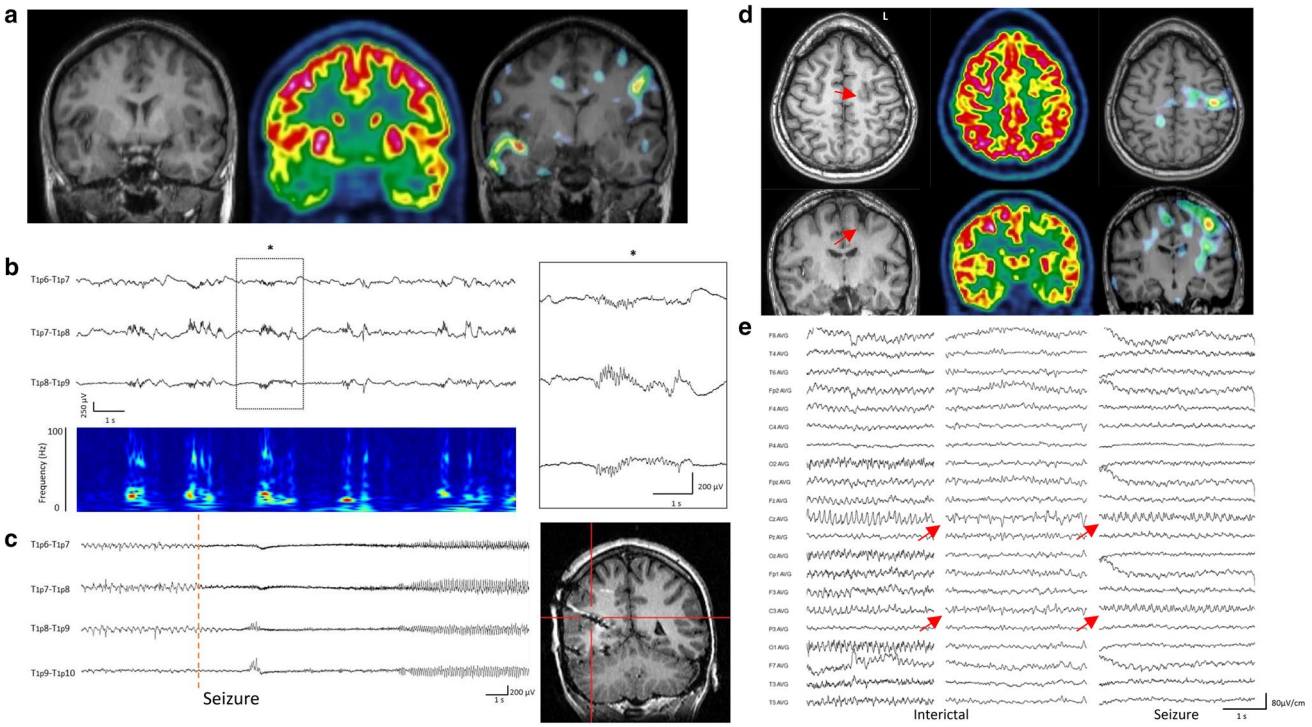

Fig. 1 Imaging, metabolic and electrophysiological features of two epileptic patients with a final diagnosis of FNL. **a**, Brain MRI and metabolic imaging from patient 1. Left panel: anatomical T1WI MRI showing no obvious lesion. Middle Panel: interictal PET showing hypometabolism in the right temporal lobe. Right panel: ictal versus interictal SPECT showing an area of hyperperfusion in the right temporopolar cortex, in particular within the superior temporal gyrus. The radiotracer was injected 27 s after the seizure onset. **b**, Interictal pattern recorded from contacts 6 to 9 of the intracerebral electrode located in the right superior temporal gyrus (see brain location on the right part of panel **c**). Interictal activity consisted of periodic discharges of fast oscillations superimposed on isolated or repetitive slow waves, sometime entangled with isolated epileptic spikes. The insert shows a magnification of the sEEG trace enclosed in the dotted rectangle. T1p: *T1* superior temporal gyrus, *p* posterior. sEEG signals are showed in bipolar montage. Lower panel: Time–Frequency Analysis (TFA) of interictal sEEG signal showed overhead (T1p7–8 channel). TFA showed periodic modulation of frequency power at around 30 Hz together with spots of higher frequency power up to 80 Hz. **c**, Left panel: Representative trace of a seizure from patient 1. Seizures were found to originate from brain tissue around the contacts 6–7-8 of the electrode T1p, and consisted of a low voltage fast activity. Right panel: Anatomical MRI showing the trajectory of the intracerebral electrode exploring the posterior part of the right superior temporal lobe. **d**, Brain MRI and metabolic imaging from patient 2. Left, upper and lower panel: axial and coronal view of brain T1WI MRI. Discrete focal blurring of the cortico-subcortical junction of the bottom of the superior left frontal sulcus (red arrow). Middle, upper and lower panel: axial and coronal view of the ^{18}FDG-PET showing hypometabolism of the left superior frontal sulcus. Right, upper and lower panel: axial and coronal view of the ictal versus interictal SPECT disclosing an area of cortical hyperperfusion centered on the lesion and the left inferior pre-central cortex. **e**, Representative traces of interictal and ictal scalp EEG of patient 2. EEG showed intermittent low amplitude rhythmic spiky activity at 6–7 Hz, on the left fronto-central and anterior midline electrodes (left panel). Interictal activity can also acquire a pseudoperiodic, short interval, appearance (middle panel). During seizures (right panel), the rhythmic ictal abnormalities showed a peculiar "sawtooth" morphology. EEG signals are showed with an average reference montage

and the pericentral region (Fig. 1a, middle panel). Ictal versus interictal SPECT (SISCOM) disclosed a hyperperfused area in the right temporopolar cortex, predominating in the superior temporal gyrus (STG; Fig. 1a right). In patient 2, brain MRI demonstrated a focal blurring at the cortico-subcortical junction of the bottom of the superior left frontal sulcus (Fig. 1d, left panel). This lesion was hypometabolic on ^{18}FDG-PET (Fig. 1d, middle). Ictal versus interictal SPECT disclosed a cortical hyperperfusion involving the lesion, extending to the homolateral inferior pre-central cortex (Fig. 1d, right panel).

EEG investigations

In patient 1, surface EEG disclosed spikes and sharp waves on the right temporal lobe. Based on the electrophysiological and metabolic features, the patient 1 underwent to a first intracranial investigation (stereoelectroencephalography, SEEG) exploring the left lateral and antero-basal temporal cortices, the left temporal pole, the left amygdalohippocampal complex and entorhinal cortex. Left orbitofrontal cortex was also explored. This SEEG investigation did not identify the origin of seizures, pointing to a more posterior location of the seizure onset zone (SOZ). A second SEEG investigation explored the posterior part of the left temporal lobe, the temporo-occipital junction and the left inferior parietal lobule (Supplementary Fig. 1). This latter SEEG investigation identified a highly active focus of interictal epileptiform discharges in the posterior part of the right STG (Fig. 1b). They consisted of quasi-continuous periodic spikes and spikes and waves with superimposed short-lasting bursts of fast activity during wakefulness. The latter increased dramatically during non-REM sleep, and appeared as short-interval (1–2 s), periodic discharges at 80 Hz oscillations (brushes), alternating with transient suppression of background activity (Fig. 1b). Recorded seizures consisted of a low voltage fast activity at seizure onset and originated from the same contacts where the interictal discharges (IIDs) were identified. (Fig. 1c). In patient 2, scalp EEG showed quasi-continuous rhythmic (6–7 Hz), low amplitude spikes/sharp waves interictal epileptiform discharges, on the left fronto-central electrodes (Fig. 1e). Seizures mainly occurred during sleep and consisted of a left frontocentral rhythmic ictal activity with a "sawtooth" morphology (Fig. 1e, right panel).

Surgery outcome

In patient 1, surgical cortectomy removed the posterior part of right STG (Fig. 2a, left right part). In patient 2, surgery removed the bottom of the posterior part of the superior left frontal sulcus (Fig. 2b, right panel). No significative reduction of seizure frequency was achieved after one year since surgery (ILAE Class 5) in both patients. These results are in line with previous observation on FNL surgery [1].

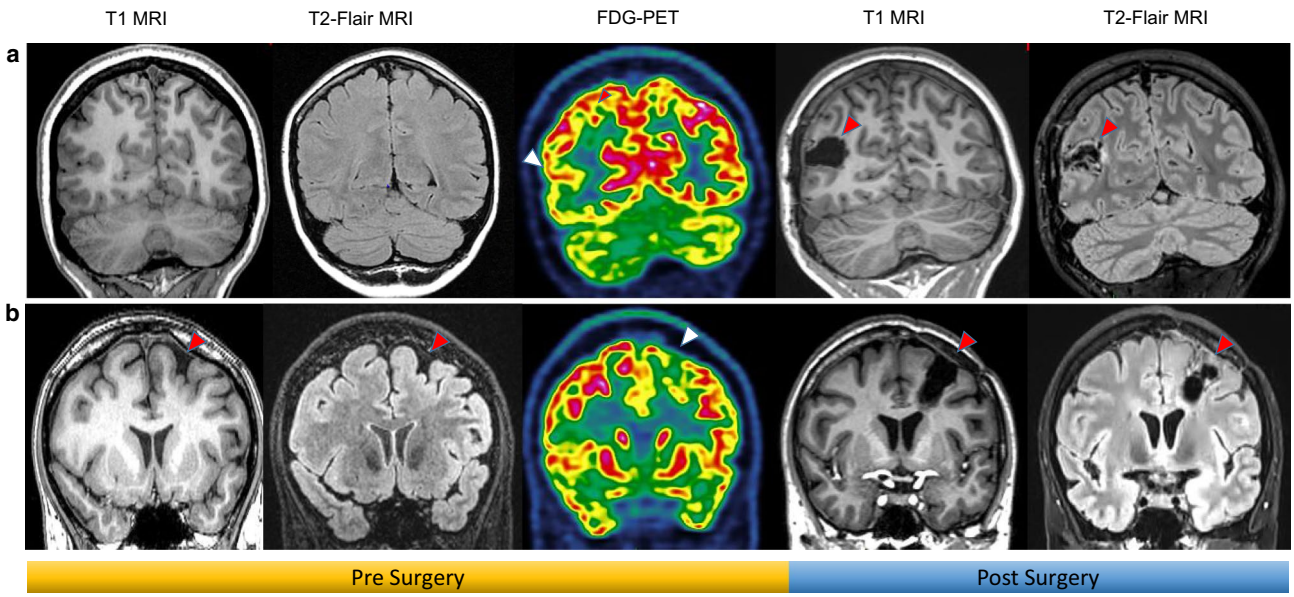

Fig. 2 Pre and Post-surgery neuroimaging showing the postsurgical cavity. **a** (from the left to the right): presurgical T1WI and T2 Flair WI from patient 1, showing no evident macroscopic focal lesion. Interictal ^{18}FDG-PET showing the posterior part of the right temporal hypometabolism. Post-surgery T1WI and T2 Flair MRI showing the post-surgical cavity located in the posterior part of right STG. **b**, Presurgical T1WI and T2 Flair WI from patient 2, showing a focal blurring at the cortico-subcortical junction of the bottom of the superior left frontal sulcus. Interictal ^{18}FDG-PET showing a focal hypometabolism associated to the lesion. Post-surgery T1WI and T2 Flair MRI showing the post-surgical cavity located in the bottom of the posterior part of the superior left frontal sulcus

Both patients underwent a second surgical intervention to remove the tissue surrounding the previous postsurgical cavity. These surgeries did not modify seizure frequency in both patients after the following months.

Neuropathological study

In both patients, neuropathological analysis of first postsurgical specimens disclosed enlarged, pyramidal or globoid neurons resembling DANs (Fig. 3a). The cytoplasm of DANs was markedly distended, showing intracellular granular material on hematoxylin–eosin. Granular material was both PAS and Luxol blue positive, suggesting excessive lipofuscin accumulation (Fig. 3b). All DANs were negative for anti-GAD staining, suggesting that they were not interneurons (Fig. 3b). p62—a protein involved in ubiquitin-proteasome system and in autophagy [5, 6]—was weakly expressed in DANs, in contrast to the strong expression found in abnormal cells of FCDIIb (Fig. 3a) [1]. The somata of lipofuscin-containing DANs were surrounded by crown-like, GAD-immunopositive puncta, compatible with peri-somatic GABAergic presynaptic buttons (Fig. 3b and c). Interestingly, no normal pyramidal neuron in the specimen showed a similar morphological feature (Fig. 3b). In both patients, lipofuscin-containing neurons showed a heterogeneous distribution within the resected tissues. Some lipofuscin-containing DANs were organized in clusters while others appeared as isolated cells. The resected tissue was fragmented, which did not allow to control the presence of neuronal lipofuscinosis at margins of the resections. The neuropathological examination of cerebral specimens after second surgery showed rare lipofuscine-containing neurons for patient 1 and no pathological neuron for patient 2.

In vitro electrophysiological recordings from post-surgery human tissue from patient 1

To correlate these morphological features with neuronal activity, we next performed in vitro recordings from the second postsurgical specimens from patient 1 using multielectrode arrays. Spontaneous, periodic (1.2 Hz), interictal-like discharges (IILDs) were identifiable in a restricted area of the slice (red electrodes in Fig. 4a). Upon application of a pro-convulsive extracellular solution (9 mM K+; 0.25 mM

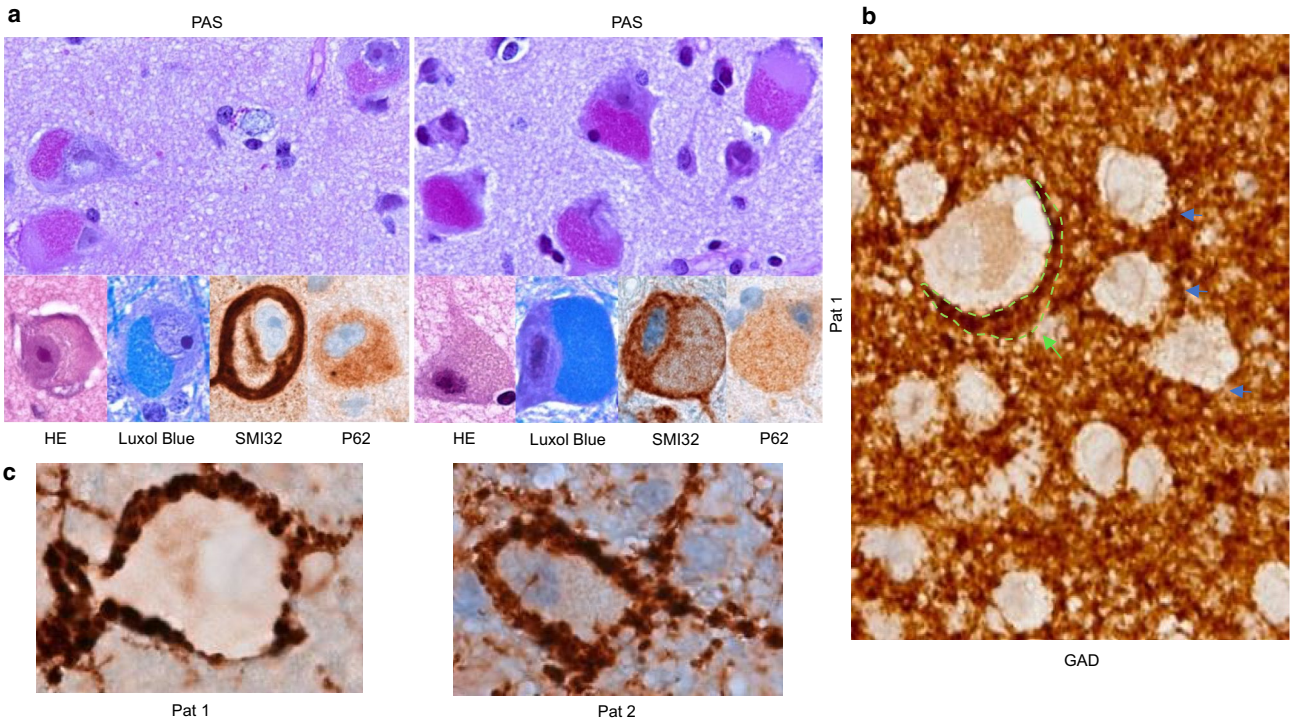

Fig. 3 Neuropathological analysis of the postsurgical specimen from Patient 1 and 2. **a**, Upper pictures: periodic Acid Schiff (PAS) coloration. In both patients dysmorphic-appearing neurons (DANs) showed intracytoplasmic granular accumulation on PAS. Lower pictures: intracytoplasmic granular accumulation was also stained by hematoxylin–eosin and displayed Luxol blue positivity, all suggesting of lipofuscin material. DANs showed strong ring-like labeling with anti-neurofilament SMI32 antibodies. DANs showed a weak positivity for p62. **b**, Anti-GAD staining revealed that DANs neurons are not inhibitory cells. DANs were surrounded by multiple extracellular, perisomatic puncta, compatible with presynaptic GABAergic boutons. This finding was observed only around DANs (dotted green lines with arrow), and not around neurons of normal appearance (blue arrows). **c**, Perisomatic GABA staining of the DANs was found in both patients

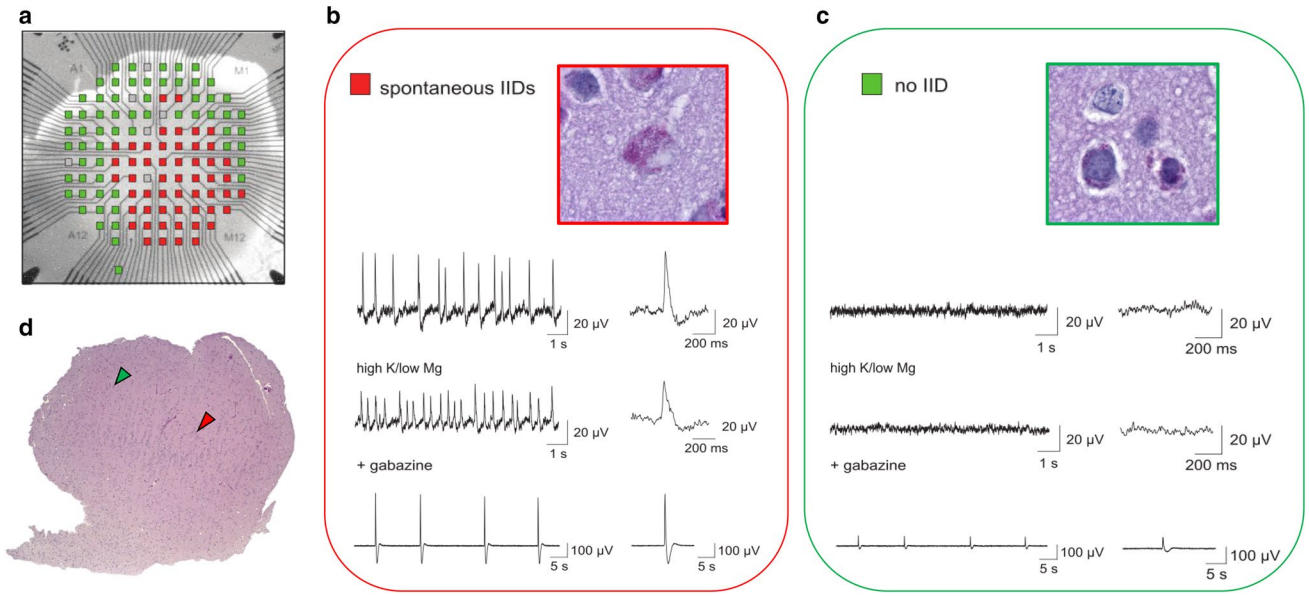

Fig. 4 Gabazine suppresses spontaneous interictal-like discharges (IILDs) recorded in vitro in human FNL tissue. **a**, Example of a cortical slice from a post-operative tissue, recorded on a 120-channel multielectrode array. The schematic representation of the electrode layout is superimposed on the image of the slice. Electrodes recording spontaneous IILDs are shown in red whereas those without IILDs are shown in green. Noisy electrodes are represented in grey and were not used for recording. Note that the epileptogenic zone is restricted to a portion of the slice. **d**, Same slice as in A, stained with PAS for lipofuscin visualization. Arrows indicate the sites from which insets in panels **b–c** were obtained. **b–c**, Representative local field potential recordings from both spontaneously active (**b**, red) and inactive (**c**, green) areas from the slice shown in panels **a–d**. Insets, magnification of the areas indicated with red (**b**) and green (**c**) arrows, respectively, in panel **d**. Note the presence of a dysmorphic neuron containing a strong intracytoplasmatic lipofuscin staining (purple) in the spontaneously active area. Top traces, spontaneous IILDs represented on different timescales, recorded from a red (**b**) but not a green (**c**) electrode. Middle traces, upon perfusion with a pro-convulsive solution (9 mM K+, 0.25 mM Mg2+, 1.6 mM Ca2+), the frequency of IILDs increased while their amplitude was reduced. No activity was induced in areas without spontaneous IILDs. Lower traces, upon addition of gabazine (10 µM), IILDs were suppressed and replaced with large amplitude, rhythmic, LFP oscillations spreading throughout the slice

Mg2+, 1.6 mM Ca2+), the frequency of IILDs increased by 27% whereas their amplitude decreased by 58% (Fig. 4b). However, no ictal-like activity was induced outside the spontaneously active area. Importantly, this area also displayed the highest density of lipofuscin-containing DANs (Fig. 4b, red arrow; Fig. 4c, red contoured square) which were virtually absent from the silent areas (Fig. 3b, green arrow; Fig. 4d, green contoured square). These findings suggest a correlation between the density of lipofuscin-containing neurons and epileptogenicity. Finally, since DANs were surrounded by a high density of putative perisomatic GABAergic synaptic boutons, we tested the role of GABA signaling in the generation of epileptic activity. Thus, application of the specific GABAA receptor antagonist gabazine (10 µM) resulted in the complete suppression of epileptiform activity detected on previously active electrodes and the emergence of slow, high-amplitude LFP oscillations in the whole slice.

Discussion

FNL is a rare and recently described pathology [1, 2]. According to the reports of a total of seven patients, FNL was systematically located in the frontal lobes. Here, we report that FNL can also be identified in the temporal lobe, as shown in one of our two patients. Previous reports did not provide details on EEG findings. Here, we report, in both patients, strikingly focal and rich interictal EEG activities. They consisted of focal rhythmic or periodic interictal epileptiform discharges resembling those described in FCDIIb [7, 8]. However, in line with the previous reports on FNL [1], surgical outcome was not satisfying in our two patients, when compared to that observed with FCD patients [1, 2, 8]. It is not clear whether these differences are due to a greater difficulty in

correctly delineating and resecting the affected tissue or to differences in network organizations around the lesion as compared with FCDIIb. Neuropathological examination of post-operative tissues from both patients showed intraneuronal lipofuscin accumulation within dysmorphic neurons, a hallmark of FNL. In line with a previous report, post-surgical tissues from our patients revealed a cortical and juxtacortical location of FNL 1 [1, 2]. Contrary to FCDIIb, lipofuscin-containing DANs were less clustered, appearing as small group of pathological cells as well as isolated ones. In addition, all DANs were GAD-immunonegative, suggesting they were not GABAergic interneurons (Fig. 3c). In contrast, their soma were surrounded by a crown-like zone of dense GABAergic presynaptic buttons. This suggested GABAergic interneurons may either contribute to the epileptogenicity of FNL or, impose an inhibitory restraint to the propagation of epileptiform activity [12–14], or both. A similar organization was reported in FCDIIb, where interneurons provide increased GABAergic innervation of DANs [9, 10]. In addition, hypertrophic basket formations established by putative parvalbumin interneurons also surround DANs in FCDs [11]. The contribution of GABAergic interneurons to epileptic activity is, however, a highly dynamic and multifaceted process. Thus, whereas GABA-mediated inhibition may prevent the spread of epileptic activity [12–14], GABAA receptor-mediated currents can also paradoxically promote epileptiform activity [15] due to altered neuronal chloride homeostasis resulting in depolarizing and excitatory GABA signaling [20, 21]. Consistent with this scenario, spontaneous seizure generation in vivo was associated with increased GABAergic interneuron activity preceding pyramidal neuron activity [16]. In human FCD tissue recorded in vitro, epileptiform activity was initiated by synchronizing mechanisms relying on GABAA receptors [16–19]. Our in vitro data from FNL resective tissue demonstrate that the epileptogenic zone is confined within a highly restricted area enriched in lipofuscin-rich neurons. In addition, we showed that spontaneous IILDs were blocked by the GABAA receptor antagonist gabazine which, however, induced widespread, large amplitude LFP oscillations beyond the limits of the spontaneously active area. These observations suggest GABA signaling in FNL tissue may both contribute to the generation of interictal-like activity and constrain the spreading of synchronous, epileptiform activity. In conclusion, we suggest that FNL is not exclusive of FLE but can be found in other types of focal epilepsies such as temporal lobe epilepsy. Although FNL and FCDIIb represent two distinct pathologies, they share some neuropathological and electrophysiological features. Histological analyses reveal an abnormal density of GABAergic terminals around the soma of lipofuscin-containing DANs, suggesting a role of GABAergic interneurons in epileptic activities. In vitro electrophysiological recordings from resected tissue further supported this hypothesis.

Supplementary Information The online version contains supplementary material available at https://doi.org/10.1007/s00415-022-11024-y.

Funding This work received support from the "Investissements d'avenir" program ANR-10-IAIHU06, and from the Fondation Assistance Publique Hôpitaux de Paris (EPIRES—Marie Laure PLV Merchandising)

Declarations

Conflicts of interest On behalf of all authors, the corresponding author states that there is no conflict of interest. We confirm that we have read the journal's position on issues involved in ethical publication and affirm that this report is consistent with those guidelines. Valerio Frazzini, Bertrand Mathon, Florian Donneger, Louis Cousyn, Aurélie Hanin, Vi-Huong Nguyen-Michel, Claude Adam, Virginie Lambrecq, Jean Christophe Poncer reports no disclosure. Sophie Dupont reports fees from Boards with UCB Pharma, EISAI, Liva Nova, GW Pharma, Takeda, Novartis. Franck Bielle reports funding of research out of the scope of this article by Abbvie, a next-of-kin employed by Bristol-Myers Squibb, fees of travel and conference out of the scope of this article by Bristol-Myers Squibb, Vincent Navarro reports fees from Boards with UCB Pharma, EISAI, Liva Nova, GW Pharma.

Ethical approval The study was performed in accordance with the ethical standards as laid down in the 1964 Declaration of Helsinki and its later amendments or comparable ethical standards.

References

1. Liu JY, Reeves C, Diehl B et al (2016) Early lipofuscin accumulation in frontal lobe epilepsy. Ann Neurol 80(6):882–895
2. Mhatre R, Jagtap SA, Kurwale N, Santhoshkumar R, Deshmukh Y, Mahadevan A (2020) Frontal lobe epilepsy with focal neuronal lipofuscinosis—case report of a rare entity. Epilepsy Behav Rep. 14:100369
3. Blümcke I, Thom M, Aronica E et al (2011) The clinicopathologic spectrum of focal cortical dysplasias: a consensus classification proposed by an ad hoc task force of the ILAE diagnostic methods commission. Epilepsia 52(1):158–174
4. Cuschieri S (2019) The STROBE guidelines. Saudi J Anaesth 13(1):S31–S34
5. Iyer A, Prabowo A, Anink J et al (2014) Cell injury and premature neurodegeneration in focal malformations of cortical development. Brain Pathol 24:1–17
6. Ichimura Y, Komatsu M (2010) Selective degradation of p62 by autophagy. Semin Immunopathol 32:431–436
7. Epitashvili N, San Antonio-Arce V, Brandt A et al (2018) Scalp electroencephalographic biomarkers I epilepsy patients with focal cortical dysplasia. Ann Neurol 84(4):564–575
8. Tassi L, Garbelli R, Colombo N et al (2012) Electroclinical, MRI and surgical outcomes in 100 epileptic patients with type II FCD. Epileptic Disord 14(3):257–266
9. Garbelli R, Munari C, De Biasi S, Vitellaro-Zuccarello L, Galli C, Bramerio M, Mai R, Battaglia G, Spreafico R (1999) Taylor's cortical dysplasia: a confocal and ultrastructural immune histochemical study. Brain Pathol 9:445–461

10. Tassi L, Colombo N, Garbelli R, Francione S, Lo Russo G, Mai R, Cardinale F, Cossu M, Ferrario A, Galli C, Bramerio M, Citterio A, Spreafico R (2002) Focal cortical dysplasia: neuropathological subtypes, EEG, neuroimaging and surgical outcome. Brain 125:1719–1732
11. Alonso-Nanclares L, Garbelli R, Sola RG, Pastor J, Tassi L, Spreafico R, DeFelipe J (2005) Microanatomy of the dysplastic neocortex from epileptic patients. Brain 128:58–173
12. Schevon CA, Weiss SA, McKhann G, Goodman RR, Yuste R, Emerson RG (2012) Evidence of a inhibitory restraint of seizure activity in humans. Nat Commun 3:1060
13. Trevelyan AJ, Sussillo D, Watson BO, Yuste R (2006) Modular propagation of epileptiform activity: evidence for an inhibitory veto in neocortex. J Neurosci 26(48):12447–12455
14. Trevelyan AJ, Sussillo D, Yuste R (2007) Feedforward inhibition contributes to the control of epileptiform propagation speed. J Neurosci 27:3383–3387
15. Avoli M, de Curtis M (2011) GABAergic synchronization in the limbic system and its role in the generation of epileptiform activity. Prog Neurobiol 95(2):104–132
16. Elahian B, Lado NE, Mankin E, Vangala S, Misra A, Moxon K, Fried I, Sharan A, Yeasin M, Staba R, Bragin A, Avoli M, Sperling M, Engel J, Weiss SA (2018) Low-voltage fast seizures in humans begin with increased interneuron firing. Ann Neurol 84(4):588–600
17. Andre VM, Flores-Hernandez J, Cepeda C, Starling AJ, Nguyen S, Lobo MK, Vinters HV, Levine MS, Mathern GW (2004) NMDA receptor alterations in neurons from pediatric cortical dysplasia tissue. Cereb Cortex 14:634–646
18. Cepeda C, Chen JC, Wub JY, Fisher RS, Vinters HV, Mathern GW, Levine MS (2014) Pacemaker GABA synaptic activity may contribute to network synchronization in pediatric cortical dysplasia. Neurobiol Dis 62:208–217
19. Avoli M, Louvel J, Mattia D, Olivier A, Esposito V, Pumain R, D'Antuono M (2003) Epileptiform synchronization in the human dysplastic cortex. Epileptic Disord 5(Suppl 2):45–50
20. Lévesque M, Ragsdale D, Avoli M (2019) Evolving mechanistic concepts of epileptiform synchronization and their relevance in curing focal epileptic disorders. Curr Neuropharmacol 17(9):830–842
21. Cohen I, Navarro V, Clemenceau S, Baulac M, Miles R (2002) On the origin of interictal activity in human temporal lobe epilepsy in vitro. Science 298:1418–1421